

# Compositional Fluctuation Region in the Ternary Solid Solution of $\text{PbZrO}_3$ - $\text{PbTiO}_3$ - $\text{Pb}(\text{CO}_{1/3}\text{Nb}_{2/3})\text{O}_3$ System

Yoshiyuki Abe,<sup>a\*</sup> Ichiro Tanaka,<sup>b</sup> Kazuyuki Kakegawa<sup>b</sup> and Yoshinori Sasaki<sup>b</sup>

<sup>a</sup>Graduate School of Science and Technology, Chiba University, Yayoi-cho Inage-ku Chiba-shi 263–8522, Japan

<sup>b</sup>Faculty of Engineering, Chiba University, Yayoi-cho Inage-ku Chiba-shi 263–8522, Japan

(Received 22 October 1997; accepted 4 March 1998)

## Abstract

A method was developed to determine a compositional fluctuation region in the ternary solid solution system  $\text{PbZrO}_3$ - $\text{PbTiO}_3$ - $\text{Pb}(\text{Co}_{1/3}\text{Nb}_{2/3})\text{O}_3$  (PZTCN) in the tetragonal region. The compositional fluctuation in the ternary system extends two-dimensionally on the phase diagram. The method described in this paper utilized the fact that the compositional fluctuation region extends to the curves of composition whose lattice spacing corresponds to the higher or lower fluctuation limit. The fluctuation limits of the lattice spacings were estimated from X-ray diffraction analysis. This method revealed that PZTCN prepared by a conventional dry method (mixed oxide method) had a considerably large compositional fluctuation. © 1998 Elsevier Science Limited. All rights reserved

## 1 Introduction

The perovskite solid solution system  $\text{PbZrO}_3$ - $\text{PbTiO}_3$  (PZT) exhibits many excellent electric properties. The large dielectric and piezoelectric constants of PZT are found near the morphotropic phase boundary (MPB),<sup>1</sup> which exists near 53.5 mol% of  $\text{PbZrO}_3$  content.<sup>2</sup> In ternary solid solutions between PZT and another complex perovskite compound, the MPB extends along a line on the phase diagram.<sup>3,4</sup> Therefore, various useful properties can be obtained among the various compositions along the MPB line.

Generally, solid solutions tend to have a compositional fluctuation. It is known that many solid solutions with the perovskite structure also have

a compositional fluctuation. The fluctuation is especially large when they were fabricated using a conventional dry method (mixed-oxide method).<sup>5–7</sup>

The compositional fluctuation in the ternary system is represented as a two-dimensional region on the ternary diagram. The electric properties depend on both the size and shape of the region, which depend on the condition of synthesis. Therefore, it is essential to establish a method to determine the compositional fluctuation region in the diagram. The relation between the region and synthetic conditions should be clarified. However, methods for the determination of the compositional fluctuation has not been studied well. In the previous papers, we reported the methods for the determination of the compositional fluctuation in the ternary solid solutions of  $\text{PbZrO}_3$ - $\text{PbTiO}_3$ - $\text{Pb}(\text{Mg}_{1/3}\text{Ta}_{2/3})\text{O}_3$ ,<sup>8</sup>  $\text{PbZrO}_3$ - $\text{PbTiO}_3$ - $\text{Pb}(\text{Mg}_{1/3}\text{Nb}_{2/3})\text{O}_3$ ,<sup>9</sup>  $\text{PbZrO}_3$ - $\text{PbTiO}_3$ - $\text{Pb}(\text{Mg}_{1/2}\text{W}_{1/2})\text{O}_3$ .<sup>10</sup>

The ternary solid solution of  $\text{PbZrO}_3$ - $\text{PbTiO}_3$ - $\text{Pb}(\text{Co}_{1/3}\text{Nb}_{2/3})\text{O}_3$  (PZTCN) is well-known as the material that exhibits high dielectric constants (750–1500) and high radial coupling coefficients (40–45%)<sup>4</sup> near the MPB. This paper describes the method to determine the compositional fluctuation region in PZTCN.

## 2 Experimental Procedure

### 2.1 Sample preparation

Samples were prepared in the following manner. Reagent-grade powder of  $\text{PbO}$ ,  $\text{ZrO}_2$ ,  $\text{TiO}_2$ ,  $\text{CoO}$  and  $\text{Nb}_2\text{O}_5$  in appropriate proportions were carefully blended and mixed thoroughly with an agate mortar and pestle. The mixtures were pressed into powder compacts. The powder compacts were sintered in a double closed magnesia crucible<sup>9</sup> with a pellet of equimolar mixture of  $\text{PbO}$  and  $\text{ZrO}_2$  as a source of  $\text{PbO}$  vapor. For a measurement of the

\*To whom correspondence should be addressed.

lattice constants the powder compacts were sintered at 1200°C for 1 h.

## 2.2 X-ray diffraction analysis

The powder X-ray diffraction data for the fired samples were obtained with Ni filtered CuK $\alpha$  radiation. In order to determine the lattice constants of tetragonal PZTCN, the 002 and 200 diffraction lines were chosen and pure Si powder (99.99%) was used as an internal standard to calibrate the systematic errors in the peak position.

The fluctuation of lattice spacings were determined for the widths of the 00 $l$ ,  $hk0$ ,  $h0h$ , and 102 diffraction peaks. These peak profiles were fitted to the following equation using the least-squares analysis:

$$I(2\theta) = A / \left\{ 1 + B(2\theta - C)^2 \right\} + 0.5A / \left\{ 1 + B(2\theta - C - \delta)^2 \right\}$$

where  $I(2\theta)$  is the intensity at an angle  $2\theta$ ,  $\delta$  is the line splitting by the doublet of CuK $\alpha_1$  and K $\alpha_2$ , and  $A$ ,  $B$  and  $C$  are constants. By means of this fit, widths at half maximum intensity (WHI) for an X-ray of single wavelength of K $\alpha_1$  were obtained. From this method WHIs of Si were determined. The WHI of Si can be seen as a width establishing the resolving power of the apparatus. These values were plotted against  $2\theta$  in order to obtain the resolution width at any angle. The resolution width at the diffraction angle of the sample was subtracted from the WHI of the sample, resulting in a value  $\beta$ ,<sup>11</sup> which is the net width of the sample.

## 3 Method

In general lattice constants of solid solutions vary with composition. The equal lattice spacing line on ternary diagram for any lattice planes can be estimated from the relation between the composition and the lattice constants. Many tetragonal solid solutions which contain PZT have the equal lattice spacing lines whose shapes differ from lattice plane to lattice plane. This is due to the different dependencies of the length of  $a$ - and  $c$ -axes on the composition. So, the fluctuation of each lattice plane is differently affected by the compositional fluctuation.

The fluctuation of the lattice spacings can be determined from the value of  $\beta$ . The plots of  $\beta \cos \theta$  versus  $\sin \theta$  (where  $\theta$  is the Bragg angle) for diffractions from a certain plane and its higher order diffractions must theoretically be fitted on a straight line.<sup>12</sup> The slope of this line corresponds to the fluctuation of the lattice spacing,  $\Delta d/d$ . The

higher limit of fluctuation of the lattice spacing can be assumed to be  $d_0 + (\Delta d/2)$  and the lower  $d_0 - (\Delta d/2)$ , where  $d_0$  is the average lattice spacing. The compositions whose lattice spacing corresponds to the higher fluctuation limit or lower one are on a curve on the ternary diagram.

In general the compositional fluctuation obeys the normal distribution curve. So the shape of the compositional fluctuation region can be assumed to be an ellipse. The ellipse area should extend to the curves of composition that have higher or lower limit of the lattice spacing.

Innumerable ellipse regions satisfy this requirement (Fig. 1). When the curves for several planes whose equal lattice spacing lines have various shapes are drawn, the ellipse region which touches all of these curves will be limited (Fig. 2). The compositional fluctuation region can be regarded as this ellipse region.

## 4 Application of the Method

The relation between the lattice constants and composition for tetragonal Pb(Zr $_x$ Ti $_{1-x}$ ) $_{1-y}$ (Co $_{1/3}$ Nb $_{2/3}$ ) $_y$ O $_3$  is shown in Fig. 3. From this relation, equal lattice spacing lines were obtained on the diagrams (Figs 4–7). Figure 8 shows the plots of  $\beta \cos \theta$  versus  $\sin \theta$  for the 00 $l$ ,  $hk0$ ,  $h0h$  and 102 diffraction peaks of Pb(Zr $_{0.2}$ Ti $_{0.8}$ ) $_{0.8}$ (Co $_{1/3}$ Nb $_{2/3}$ ) $_{0.2}$ O $_3$  fired at 1200°C for 1 h. The plots of 00 $l$ ,  $hk0$  and  $h0h$  diffractions were fitted on straight lines, so that the slopes were estimated. The intercepts of the lines at  $\sin \theta = 0$  for all the diffractions must be theoretically the same, which depends on the crystallite size of the sample. The plots of ( $n$  0  $2n$ ) diffraction peaks ( $n \geq 2$ ) could not be obtained because of difficulty of the measurement. Thus the plot of (102) planes was linearly connected with the intercept mentioned above, and then the slope was estimated.

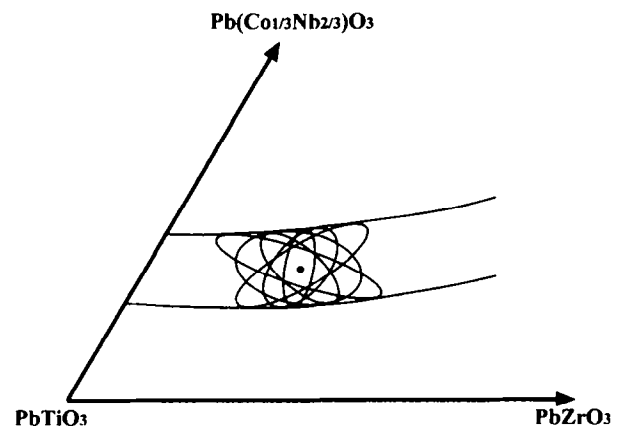


Fig. 1. Curves of compositions corresponding to the distribution limit of lattice spacing for a certain lattice plane, and the possible compositional fluctuation regions.

Figure 9 shows the curves of composition corresponding to the fluctuation limits of lattice spacings and the compositional fluctuation region ellipse estimated from these curves. The compositional fluctuation region was revealed to be considerably large. PZTCN had larger compositional

fluctuation than other ternary systems, such as  $\text{PbZrO}_3\text{-PbTiO}_3\text{-Pb}(\text{Mg}_{1/3}\text{Ta}_{2/3})\text{O}_3$ ,<sup>8</sup>  $\text{PbZrO}_3\text{-PbTiO}_3\text{-Pb}(\text{Mg}_{1/3}\text{Nb}_{2/3})\text{O}_3$ ,<sup>9</sup>  $\text{PbZrO}_3\text{-PbTiO}_3\text{-Pb}(\text{Mg}_{1/2}\text{W}_{1/2})\text{O}_3$ .<sup>10</sup> As for PZTCN, dielectric constant and radial coupling coefficient have large dependence on the composition.<sup>4</sup> This means that the electric properties can be affected greatly by the compositional fluctuation. In order to obtain the excellent electric properties from PZTCN, it is necessary to prepare the sintered body having the compositional fluctuation as small as possible.

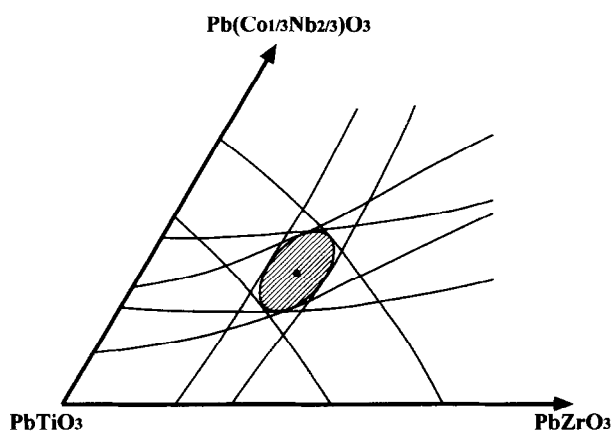


Fig. 2. Relation between a compositional fluctuation region and curves of compositions corresponding to the determination limit of lattice spacings for several lattice planes.

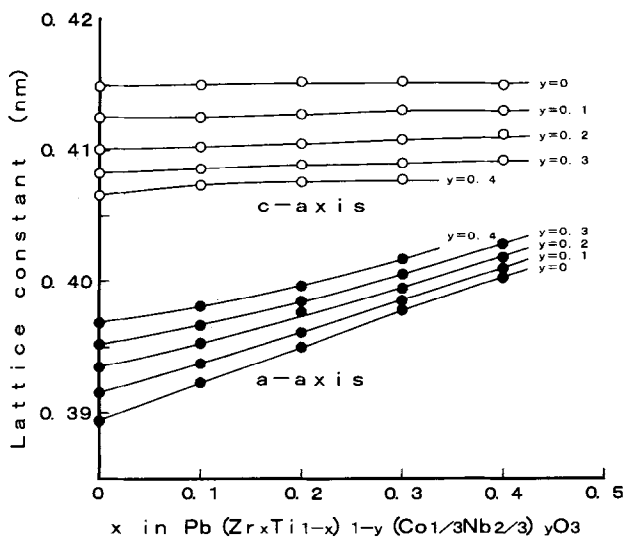


Fig. 3. Relation between lattice constants and composition for  $\text{Pb}(\text{Zr}_x\text{Ti}_{1-x})_{1-y}(\text{Co}_{1/3}\text{Nb}_{2/3})_y\text{O}_3$ .

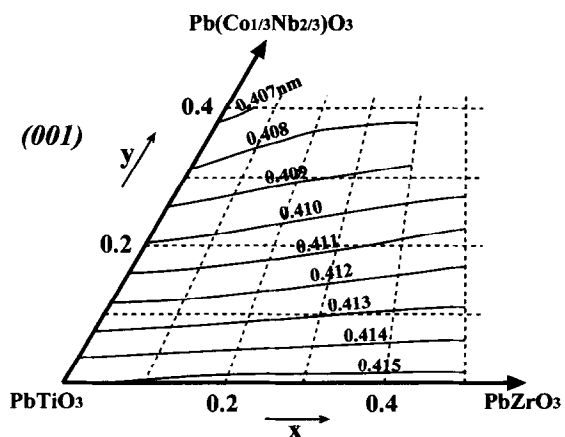


Fig. 4. Equal lattice spacing curves for (001) plane of PZTCN.

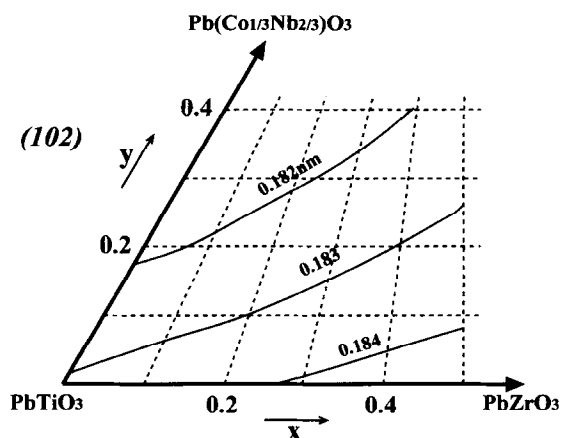


Fig. 5. Equal lattice spacing curves for (102) plane of PZTCN.

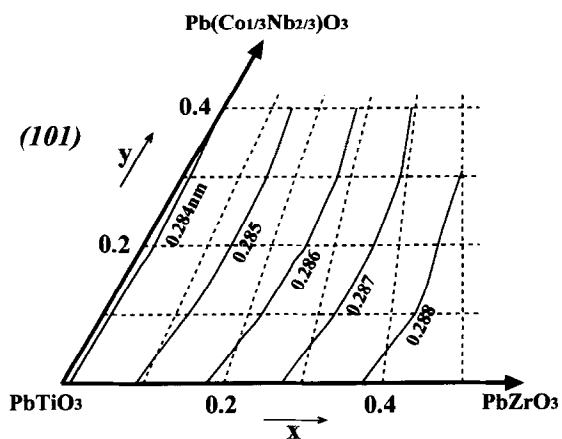


Fig. 6. Equal lattice spacing curves for (101) plane of PZTCN.

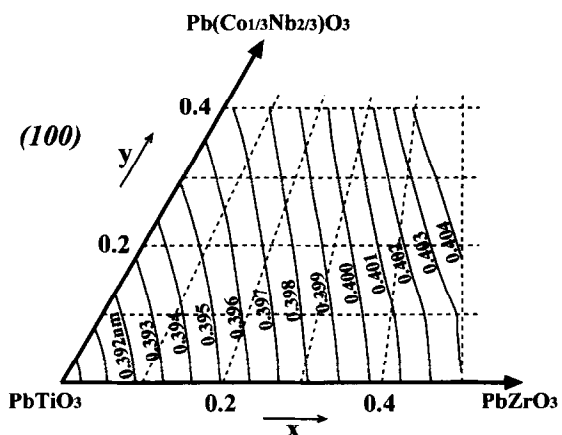


Fig. 7. Equal lattice spacing curves for (100) plane of PZTCN.

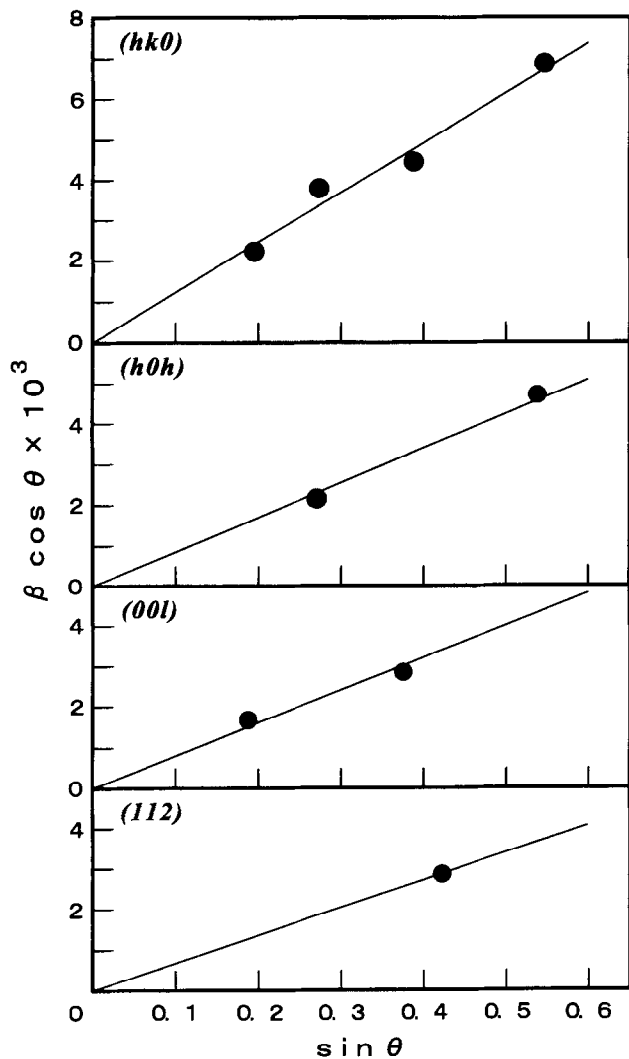


Fig. 8. Plots of  $\beta \cos \theta$  versus  $\sin \theta$  for  $\text{Pb}(\text{Zr}_{0.2}\text{Ti}_{0.8})_{0.8}(\text{Co}_{1/3}\text{Nb}_{2/3})_{0.2}\text{O}_3$  fired at  $1200^\circ\text{C}$  for 1 h.

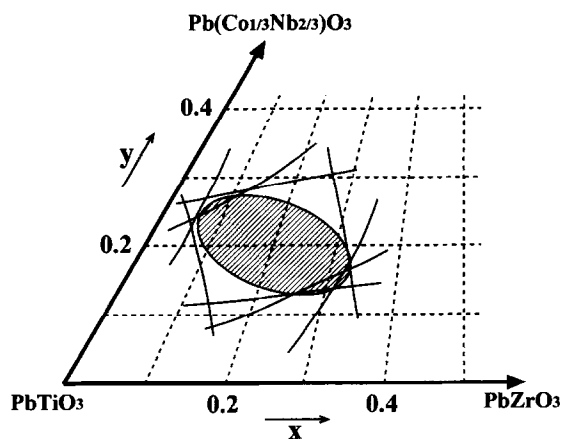


Fig. 9. Compositional fluctuation region estimated for  $\text{Pb}(\text{Zr}_{0.2}\text{Ti}_{0.8})_{0.8}(\text{Co}_{1/3}\text{Nb}_{2/3})_{0.2}\text{O}_3$  fired at  $1200^\circ\text{C}$  for 1 h.

## 5 Conclusion

The compositional fluctuation region in the ternary solid solution of  $\text{PbZrO}_3\text{-PbTiO}_3\text{-Pb}(\text{Co}_{1/3}\text{Nb}_{2/3})\text{O}_3$  system could be determined by a measurement of width of several X-ray diffraction peaks. The shape of the equal lattice spacing lines of PZTCN differed from lattice plane to lattice plane, as well as the other ternary system investigated previously. This method revealed that PZTCN prepared by a conventional dry method had a large compositional fluctuation.

## References

- Jaffe, B., Roth, R. S. and Marzullo, S., Piezoelectric properties of lead zirconate-lead titanate solid-solution ceramics. *Journal of Appl. Phys.*, 1954, **25**, 809-810.
- Kakegawa, K., Mohri, J., Shirasaki, S. and Takahashi, K., Sluggish transition between tetragonal and rhombohedral phases of  $\text{Pb}(\text{Zr,Ti})\text{O}_3$  prepared by application of electric field. *Journal of Am. Ceram. Soc.*, 1982, **65**, 515-519.
- Ouchi, H., Nagano, K. and Hayakawa, S., Piezoelectric properties of  $\text{Pb}(\text{Mg}_{1/3}\text{Nb}_{2/3})\text{O}_3\text{-PbTiO}_3\text{-PbZrO}_3$  solid solution ceramics. *Journal of Am. Ceram. Soc.*, 1965, **48**, 630-635.
- Kudo, T., Yazaki, T., Naito, F. and Sugaya, S., Dielectric and piezoelectric properties of  $\text{Pb}(\text{Co}_{1/3}\text{Nb}_{2/3})\text{O}_3\text{-PbTiO}_3\text{-PbZrO}_3$  solid solution ceramics. *Journal of Am. Ceram. Soc.*, 1970, **53**, 326-328.
- Kakegawa, K., Watanabe, K., Mohri, J., Yamamura, H. and Shirasaki, S., Fluctuation of composition of  $\text{Pb}(\text{Zr}_x\text{Ti}_{1-x})\text{O}_3$ . *Journal of Chem. Soc. Jpn.*, 1975, 413-416.
- Kakegawa, K., Mohri, J., Takahashi, K., Yamamura, H. and Shirasaki, S., Compositional fluctuation of  $\text{Pb}(\text{Zr}_x\text{Ti}_{1-x})\text{O}_3$  near tetragonal-rhombohedral phase-boundary. *Journal of Chem. Soc. Jpn.*, 1976, 717-721.
- Kakegawa, K., Mohri, J., Takahashi, T., Yamamura, H. and Shirasaki, S., A compositional fluctuation and properties of  $\text{Pb}(\text{Zr,Ti})\text{O}_3$ . *Solid State Commun.*, 1977, **24**, 769-772.
- Kakegawa, K., Kawakami, M. and Sasaki, Y., Determination of the compositional fluctuation in the perovskite ternary system  $\text{PbZrO}_3\text{-PbTiO}_3\text{-Pb}(\text{Mg}_{1/3}\text{Ta}_{2/3})\text{O}_3$ . *Journal of Am. Ceram. Soc.*, 1988, **71**, C444-C446.
- Kakegawa, K., Makigaki, K. and Sasaki, Y., Determination of the compositional fluctuation region in the solid solution of  $\text{Pb}[(\text{Zr}_x\text{Ti}_{1-x})_{1-y}(\text{Mg}_{1/3}\text{Nb}_{2/3})_y]\text{O}_3$ . *Journal of Ceram. Soc. Jpn.*, 1988, **96**, 681-686.
- Abe, Y., Kakegawa, K. and Sasaki, Y., Determination of the compositional fluctuation region in the solid solution of  $\text{PbZrO}_3\text{-PbTiO}_3\text{-Pb}(\text{Mg}_{1/2}\text{W}_{1/2})\text{O}_3$  system. *Solid State Commun.*, 1989, **72**, 1071-1074.
- Klug, H. P. and Alexander, L., *X-ray, diffraction procedures*. Wiley, New York, 1954, p. 500.
- Williamson, G. K. and Hall, W. H., X-ray line broadening from filed aluminum and wolfram. *Acta Metall.*, 1953, **1**, 22-31.